

ENVIRONMENTAL EFFECTS IN MIXERS AND FREQUENCY DISTRIBUTION SYSTEMS

L. M. Nelson and F. L. Walls
 Time and Frequency Division
 National Institute of Standards and Technology
 Boulder, CO 80303

Abstract

This paper examines the environmental sensitivity of key elements of measurement systems, frequency synthesizers, and frequency distribution systems designed to achieve frequency stabilities of order $\sigma_y(\tau) = 5 \times 10^{-15} \tau^{-1/2}$ in the short-term and 3×10^{-18} in the long-term. Specifically, we investigate the timing errors in signal transmission for distances up to 100 m and the effect of changes in temperature and rf amplitude on timing (or frequency) errors in several types of phase detectors operated in different configurations.

Introduction

Several new types of frequency standards have been proposed that show a potential for a short-term frequency stability of approximately $2 \times 10^{-15} \tau^{-1/2}$ and a long-term frequency stability less than 1×10^{-17} [1-4]. To measure frequency stability on this level and to construct the electronics of the local oscillator for interrogating the atomic system will require substantial improvements in key building blocks such as phase detectors within the measurement system, phase detectors used in frequency manipulation, and frequency distribution systems. To measure these new clocks, it is desirable to have a measurement system that reaches the clock performance at a measurement time no longer than 10^4 s. This requires a resolution of approximately $\sigma_y(\tau) = 2 \times 10^{-17}$ at a measurement time of 10^4 s, or a timing error of 0.2 ps. Similar timing requirements apply to the frequency synthesis within the reference source and in the frequency distribution systems. Figure 1 shows the common elements of these systems. In this paper we investigate the timing errors in signal

Contribution of the U. S. Government, not subject to copyright.

transmission over distances up to 100 m and the effect of changes in temperature and rf amplitude on timing (or frequency) errors in several types of phase detectors operated in different configurations.

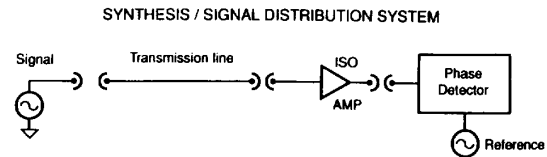


Fig. 1. Overall block diagram showing the key elements for measuring the frequency or time of a remote clock.

Timing Errors In Signal Transmission

Potentially serious timing errors can occur due to the variation of transit time delay and the phase of the standing waves on the transmission line connecting the signal (clock) to the measurement system. The transit delay of a signal is given by the length divided by the velocity of propagation. Signals transmitted to the measurement system and reflected from the load and then from the signal source lead to phase change of the signal at the load. Changes in the voltage standing wave ratio (VSWR) therefore lead to changes in timing errors. The complete timing error from transmission is

$$\delta t = L/(\beta c) + (1/(4\nu_o)) ((\rho_l \rho_s)/\eta) \sin \phi, \quad (1)$$

where L is the equivalent free space length of the transmission line, c is the speed of light, β is the propagation factor, ν_o is the carrier frequency, η is the round trip attenuation, ρ_l is the voltage reflection ratio from the load, ρ_s is the voltage reflection ratio from the source ($\rho = (VSWR - 1)/(VSWR + 1)$), and ϕ is the angle of the twice reflected wave at the

load relative to the primary signal. This assumes that the next order of reflected waves can be ignored ($(\rho_s \rho_l)/\eta \ll 1$). The first term in (1) is independent of frequency while the second term scales as $1/\nu_0$.

The variation in the timing error due to changes in $L/(\beta c)$ is potentially quite large for long transmission cables. Typical variations for several types of semi-rigid coaxial cables versus temperature are shown in Fig. 2 [5]. Typical insertion losses are of order 1 dB/30 m at 5 MHz and 3 dB/30 m at 100 MHz for 0.358 cm diameter cable. Cables with solid teflon dielectric exhibit large hysteresis effects (due to the mismatch between the thermal expansion coefficient between the dielectric and the conductors) for temperature variations from 10 to 20 °C. Various attempts have been made to produce cable with a smaller temperature sensitivity by reducing the amount of teflon dielectric or incorporating compensating materials (curves B-D of Fig. 2.). Curve E of Fig. 2 shows the temperature sensitivity of a cable that uses SiO₂ powder as the dielectric. The phase variation from 18.3 to 23.8 °C is less than ± 0.5 ps per 30 m, while the insertion loss is 3.2 dB/30 m at 100 MHz. This generally satisfies the timing requirements for distances up to approximately 100 m. The primary limitation with this cable is the cost. Except in cases where there are large temperature variations, one of the other cables from Fig. 2 usually performs acceptably at less cost for distances up to approximately 1 m. This data is summarized in Table 1.

At 5 MHz, $1/(4 \nu_0)$ is 50 ns and typical numbers for ρ_l and ρ_s are 1/3 (VSWR = 2). This can lead to large timing error variations since VSWR is often dependent on temperature, rf drive level, and even supply voltage. Significant improvements in the timing errors due to VSWR can be made by making ρ_l , ρ_s , and $\sin \phi$ small. At 5 MHz, for example, the timing error due to VSWR can be reduced below 11 ps by reducing VSWR below 1.1 at the source and load, and reducing $\sin \phi$ below 0.1. At 100 MHz this term can be made less than 1 ps by making VSWR < 1.1 and $\sin \phi < 0.1$. The characteristic impedance of coaxial cables changes slightly from one batch to another which might require a small adjustment in source and load impedances for the most critical applications.

An alternative approach to the problem is to use two-way transmission measurements to correct for variations in the transmission medium. This technique has been pursued at the Jet Propulsion Laboratory (JPL) where they have concentrated on AM modulation of a laser transmitted over fiber optic cables to solve both the attenuation of the signal and timing errors for cable lengths up to 25 km. The JPL results [6], shown in Fig. 3, are very impressive. Although this system is relatively costly, it is currently the only practical approach to long transmission distances due to the problem of attenuation.

Table 1. Timing/frequency errors due to variations in cable length with temperature.

BASIC TYPES OF CABLES	Loss/30 m @ 100 MHz DIAMETER	$\delta t/K$ 23-30°C per 30 m	APPROXIMATE COST/30 m
SOLID DIELECTRIC PTFE common semi-rigid (A)	3.4 dB 0.358 cm	1 ps	\$ 210
MICROPOROUS (B)	2.8 dB 0.483 cm	1 ps	\$4000
LOW DENSITY PTFE (C)	2.4 dB 0.358 cm	0.9 ps	\$ 550
AIR ARTICULATED PTFE (D)	2.7 dB 0.358 cm	0.4 ps	\$ 950
COMPENSATED DIELECTRIC ISOCORE (E)	3.5 dB 0.358 cm	0.18 ps	\$ 657
SiO ₂ DIELECTRIC (F)	3.2 dB 0.358 cm	0.06 ps	\$2200

Environmental Sensitivity of Phase Detectors

One measure of phase detector performance is the phase error $\delta\phi$ given by

$$\delta\phi = \delta V/k_d, \quad (2)$$

where δV is the dc output voltage error and k_d is the phase detection slope in volts/rad [5]. For comparing

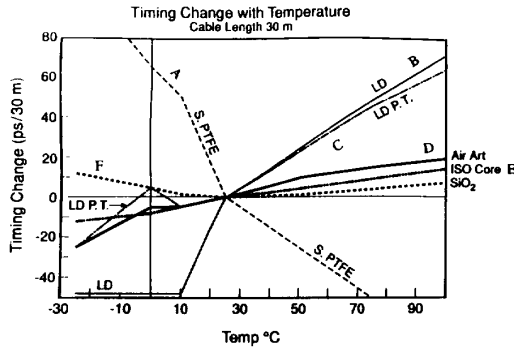


Fig. 2. Fractional phase shift versus temperature for several different semi-rigid coaxial cables. Curve A, typical .358 cm (0.141") solid teflon dielectric cable. Curve B, data for .483 cm cable with lowered teflon content. Curve C, data for .358 cm cable with lowered teflon content. Curve D, data for .358 cm air-articulated cable. Curve E, phase shift data for .358 cm cable with the temperature coefficient of the dielectric matched to the conductors. Curve F data for .358 cm cable with SiO₂ dielectric.

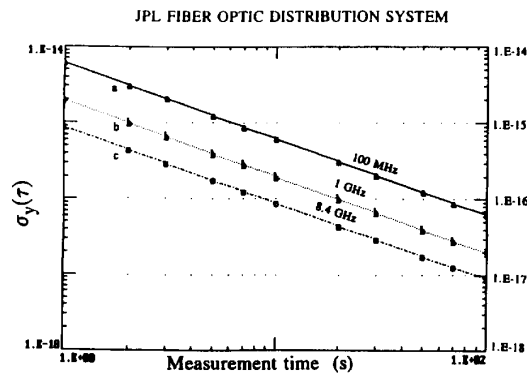


Fig. 3. Fractional timing error versus measurement time of the JPL fiber optic system for AM frequencies of 100 MHz, 1 GHz, and 8.4 GHz. Timing error is $\tau\sigma_y(\tau)$.

different phase detector circuits as a function of carrier frequency, ν_o , it is more useful to use the timing error given in seconds by

$$\delta t = (\delta V/k_d) (1/(2\pi\nu_o)). \quad (3)$$

The dc voltage error originates from imbalance between the I-V curves of the diodes, imbalance in the various transformers, and asymmetric stray impedances. These imbalances are a function of the temperature and drive levels and therefore lead to changes in apparent phase or time with change in these parameters. The most important parameter that characterizes these effects is the isolation between the LO and rf ports and the IF port. Table 2 shows approximate dc offsets as a function of LO drive and isolation [7].

Table 2. DC offset voltage in mV for various combinations of LO drive level and isolation assuming a 50 Ω resistance on all ports.

		LO DRIVE LEVEL -- dBm						
		0	+3	+7	+10	+13	+17	+20
ISOLATION - dB	15	25.3	35.8	63.7	90.0	127.1	226.0	319.2
	20	14.2	20.1	35.8	50.6	71.5	127.1	179.5
	25	8.0	11.3	20.1	28.5	40.2	71.5	100.9
	30	4.5	6.4	11.3	16.0	22.6	40.2	56.8
	35	2.5	3.6	6.4	9.0	12.7	22.6	31.9
	40	1.4	2.0	3.6	5.1	7.1	12.7	17.9
	45	0.80	1.1	2.0	2.9	4.0	7.1	10.1
50	0.45	0.64	1.1	1.6	2.3	4.0	5.7	

Table 2. DC offset voltage in mV for various combinations of LO drive level and isolation assuming a 50 Ω resistance on all ports. From Watkins-Johnson Application Note [7].

Figure 4 shows a typical circuit diagram for evaluating the phase detectors. The dc output (IF) port is terminated with the characteristic impedance, which is typically 50 Ω for the double balanced mixers and 500 Ω for the single balanced mixers.

Figures 5 through 7 show timing errors in selected phase detectors due to variation in input power at two temperatures for a carrier frequency of 5 MHz [5]. One set of curves was taken without attenuators and the others with either 3 or 6 dB attenuators on the rf and LO inputs. At 5 MHz the mixer with the individually matched diodes has a temperature coefficient of approximately 6 ps/K when used with 6 dB pads, while the mixers with the quad diodes

exhibit a temperature coefficient of about 25 ps/K. The sensitivity to power changes is generally improved by adding 3 or 6 dB attenuators to the input

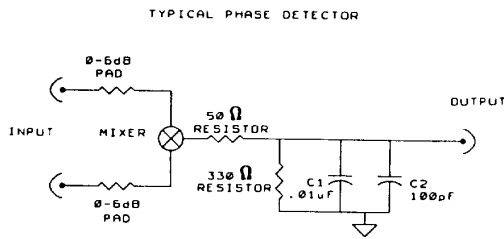


Fig. 4. Typical circuit diagram for evaluating the sensitivity of various phase detectors to variations in temperature and rf level.

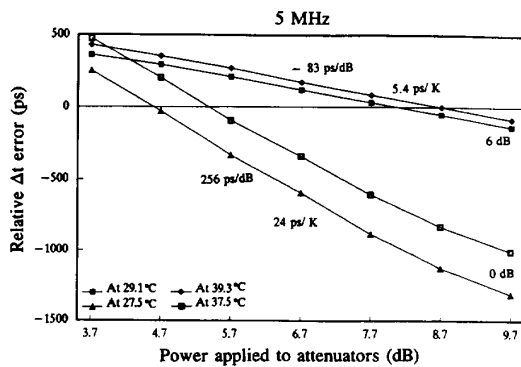


Figure 5. Timing errors in a double balanced mixer with individual discrete diodes at a carrier frequency of 5 MHz as a function of drive power, input attenuation, and temperature.

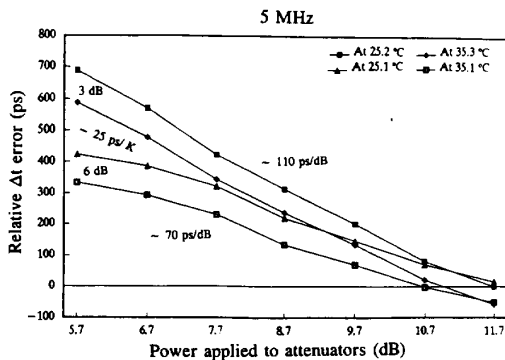


Figure 6. Timing errors in a double balanced mixer with a quad diode module, at a carrier frequency of 5 MHz as a function of drive power, input attenuation, and temperature.

ports. Without attenuators the power sensitivity is of order 1 ms/(dB ν_0) or 250 ps/dB. The improvement, due to the attenuator use on the rf and LO inputs, is thought to originate from the reduction in the cable VSWR generated by the phase detector load.

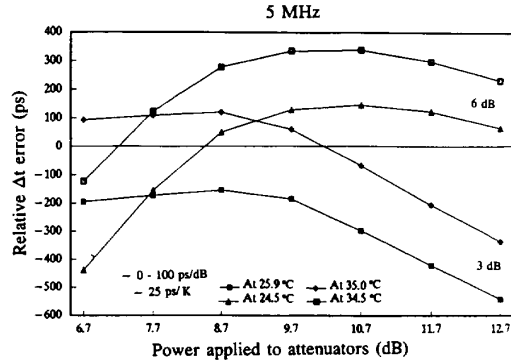


Figure 7. Timing errors in a single balanced mixer with a dual diode module, at a carrier frequency of 5 MHz as a function of drive power, input attenuation, and temperature.

Figures 8 through 10 show the timing errors in selected phase detectors due to variations in input power at two temperatures for a carrier frequency of 100 MHz [5]. One set of curves was taken without attenuators and the others with either 3 or 6 dB attenuators on the rf and LO inputs. The performance at 100 MHz of all three phase detectors versus temperature and power is improved over the results at 5 MHz by approximately the ratio of the carrier frequencies. Temperature sensitivity is of order 0.2 to 1 ps/K. The best temperature performance comes from the mixer with individually matched diodes. The power sensitivity is of order 0.1 to 1 ps/(dB ν_0) or 1 to 10 ps/dB at 100 MHz depending on mixer type, input power, and attenuation.

Figures 11 and 12 show the timing errors in a double balanced phase detector with quad diodes. This detector has been approximately matched to 50 Ω by adding an extra resistor in series with a 6 dB attenuator [5]. Timing changes due to variations in input power level and two different temperatures are shown. Figure 11 shows a set of curves taken with the added resistor at a carrier frequency of 5 MHz. The mixer has a temperature coefficient of approximately 3.5 ps/K. The power sensitivity is approximately 71.1 ps/dB and is better at higher power levels. The sensitivity to temperature is

improved greatly as compared to the data obtained without the matching as shown in Figure 6.

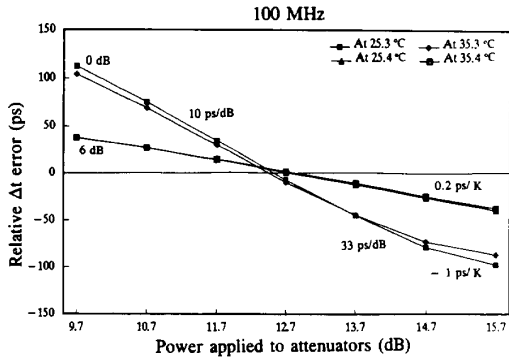


Figure 8. Timing errors in a double balanced mixer with individual discrete diodes, at a carrier frequency of 100 MHz as a function of drive power, input attenuation, and temperature.

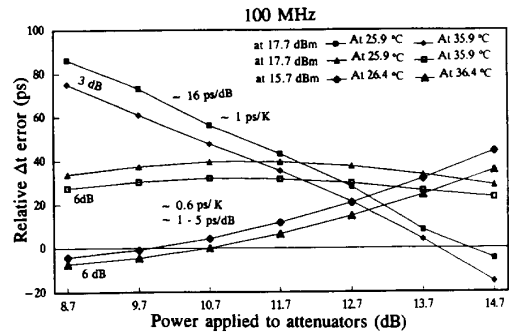


Figure 9. Timing errors in a double balanced mixer with a quad diode module, at a carrier frequency of 5 MHz as a function of drive power, input attenuation, and temperature.

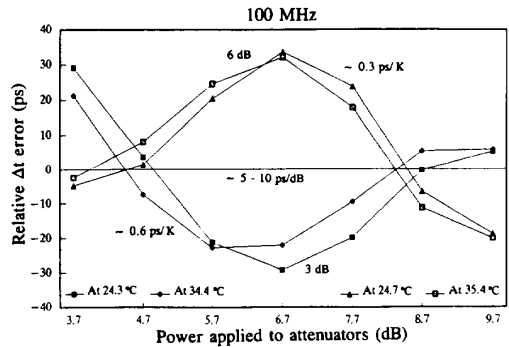


Figure 10. Timing errors in a single balanced mixer with a dual diode module, at a carrier frequency of 100 MHz as a function of drive power, input attenuation, and temperature.

5 MHz

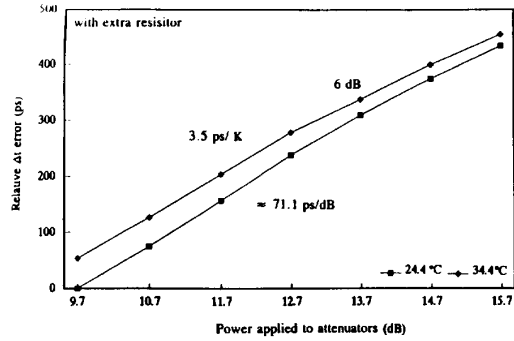


Figure 11. Timing errors in a double balanced mixer with quad diodes, at a carrier frequency of 5 MHz as a function of drive power, input attenuation (6 dB with extra resistance), and temperature.

Figure 12 shows a set of curves taken with the added resistor at a carrier frequency of 100 MHz. The mixer has a temperature coefficient of approximately 0.25 ps/K. The power sensitivity proved to be less at lower power and ranged from 1.6 ps/dB to 4 ps/dB. The extra resistor for the 50 Ω match helped to make the system less sensitive to the changes in the mixer temperature and power level. Figure 9 shows this improvement over the data taken before matching.

100 MHz

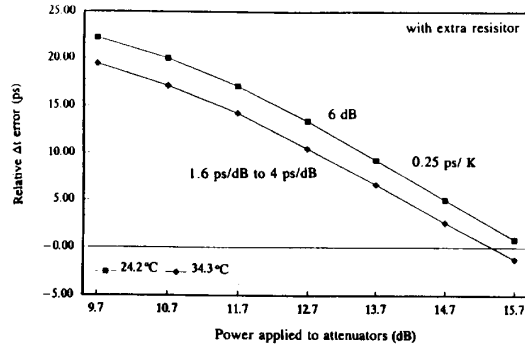


Figure 12. Timing errors in a double balanced mixer with quad diodes, at a carrier frequency of 100 MHz as a function of drive power, input attenuation (6 dB with extra resistance), and temperature.

Figures 13 and 14 show timing errors in a single balanced phase detector with an adjustable external output, a potentiometer, due to the variation in input power for two different temperatures. For a carrier frequency of 5 MHz (Figure 13), the mixer has a temperature coefficient of approximately 33 ps/K.

This is quite different from data taken for a single balanced phase detector without an adjustable external output (Figure 7). The fine tuning capabilities provide a more stable system that is less sensitive to temperature and power variations, providing a more stable system.

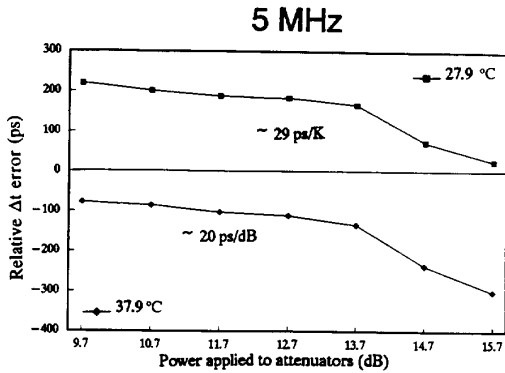


Figure 13. Timing errors in a single balanced mixer with an external adjustment, at a carrier frequency of 5 MHz as a function of drive power and temperature.

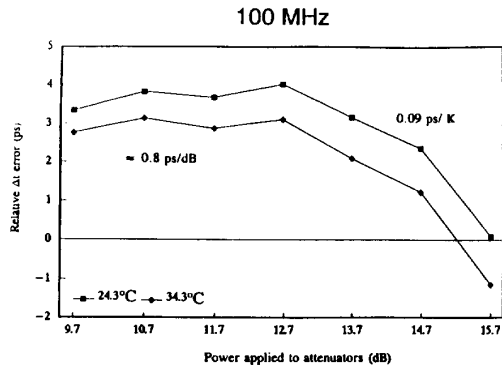


Figure 14. Timing errors in a single balanced mixer with an external adjustment, at a carrier frequency of 100 MHz as a function of drive power and temperature.

Measurements taken at 100 MHz (Figure 14) show that the phase detector has a temperature coefficient of approximately 0.09 ps/K and a power sensitivity of approximately 0.8 ps/dB. Using the external adjustment to match the diodes we were able to achieve a minimum dc offset variation between power levels which allowed for a very stable measurement of the time variation with the temperature change. Figure 10 shows data for a similar single balanced

phase detector without the external adjustment for matching capabilities.

Figures 15 and 16 show the VSWR changes in the quad diode double balanced mixer with changing rf power. For a carrier frequency of 5 MHz, shown in Figure 15, the mixer VSWR exhibits a small dependence on power when it is matched to the 50 Ω characteristic system impedance with an extra resistor added in series with the 6 dB pads on each input port. The low sensitivity of VSWR to power reduces timing error within the measurement system. At 100 MHz the mixer also has low sensitivity to changes in power when it is matched with the extra resistor (Figure 16). These results also indicate that the VSWR is better at low powers as was evident at 5 MHz (Figure 15). However, we find that there is less change in the VSWR at 100 MHz than at 5 MHz and we obtain an even smaller timing error in our measurement system.

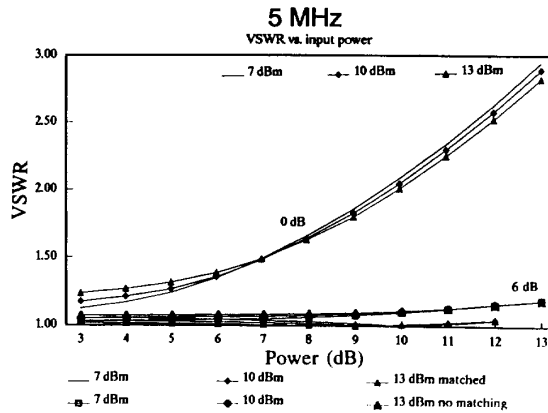


Figure 15. VSWR in a double balanced mixer with quad diodes, at a carrier frequency of 5 MHz as a function of the drive power and input attenuation (6 dB and 6 dB with extra resistance for matching).

Discussion

It is much easier to achieve the desired time domain performance of $\delta\nu/\nu_0 = \delta t/t = 2 \times 10^{-17}$ at a measurement time of 10^4 s for a carrier frequency of 100 MHz than at 5 MHz due to the sensitivity of currently available phase detectors to both temperature and rf amplitude. Even at 100 MHz it will probably be necessary to stabilize the temperature of the phase detectors to about 1 K and carefully match the characteristic impedance of the

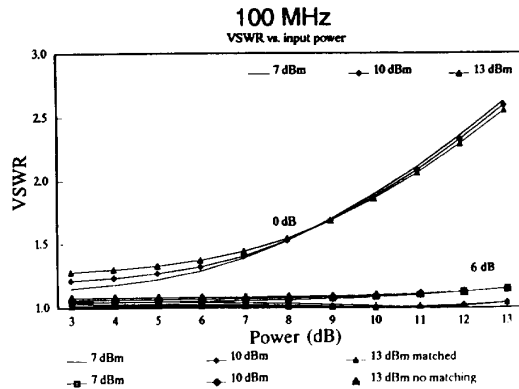


Figure 16. VSWR in a double balanced mixer with quad diodes, at a carrier frequency of 100 MHz as a function of the drive power and input attenuation (6 dB and 6 dB with extra resistance for matching).

coaxial cable. For distances of up to 100 m, existing coaxial cables are probably sufficient. For longer distances one must consider either AM modulation of a laser transmitted over fiber optic cables or using lower frequencies where the attenuation losses are smaller. The fiber optic has already demonstrated excellent performance for distances up to 25 km and is probably the best choice. Going to 5 MHz would require two-way timing measurements to correct for the time dispersion in the transmission medium and much more effort on stabilizing the operating parameters of the phase detector and lowering the effects of VSWR at the source and the load. Being able to match the diodes by using an external adjustment for tuning and matching the VSWR at the inputs seems most reasonable to accomplish the accuracy and stability that we want to achieve.

Acknowledgements

The authors would like to thank C. Osborn for help in construction details and G. Valdez for help in construction. They would also like to thank Z. Popovic for her guidance and support.

References

- [1] D. J. Wineland, J. C. Bergquist, J. J. Bollinger, W. M. Itano, D. J. Heinzen, S. L. Gilbert, C. H. Manney, and M. G. Raizen, "Progress at NIST toward absolute frequency standards using stored ions," *IEEE Trans. on Ultrasonics, Ferroelectrics, and Frequency Control*, **37**, 515-523 (1990).
- [2] J. D. Prestage, G. J. Dick, and L. Maleki, "Linear ion trap based atomic frequency standard," *Proc. of 44th Ann. Frequency Control Symp.*, 1990, pp. 82-88.
- [3] S. Chu, "Laser manipulation of atoms and particles," *Science*, **253**, 861-866 (1991).
- [4] J. L. Hall, M. Zhu, and P. Buch, "Prospects for using laser-prepared atomic fountains for optical frequency standards applications," *J. Opt. Soc. Am. B*, **6**, 2194-2205 (1989).
- [5] Certain commercial equipment, instruments, or materials are identified in this paper in order to adequately specify the experimental procedure. Such identification does not imply recommendation or endorsement by the National Institute of Standards & Technology, nor does it imply that the materials or equipment identified are necessarily the best available for the purpose.
- [6] G. F. Lutes and R. T. Logan, "Status of frequency and timing reference signal transmission by fiber optics," *Proc 45th Ann Frequency Control Symp.*, 1991, pp. 679-686.
- [7] "Mixers as phase detectors," from 1985 *Watkins-Johnson Catalog*, pp. 666-673, 1985.